IEEJ Journal of Industry Applications
Vol.6 No.2 pp.151–159 DOI: 10.1541/ieejjia.6.151

Paper

Contact Point Calculation on a Haptic Interface Utilizing Differentiated Force

Hiroyuki Kitamura[*a)] Non-member, Sho Sakaino[*] Senior Member
Toshiaki Tsuji[*] Senior Member

(Manuscript received June 11, 2016, revised Oct. 19, 2016)

In recent years, studies on haptic interfaces have progressed. This study deals with the development of the "Haptic Desk", which can detect force information and contact position information using a simple mechanism with force sensors. However this technique has low contact point accuracy when the external force is small. Hence, this paper proposes the use of differentiated force information to calculate an accurate contact point. In the experiment, the accuracy of the contact point calculation using the differentiated force information was higher than the one using the force information when the external force was small. Therefore, the error of the contact point decreased regardless of the magnitude of the force when the force information and differentiated force information were used properly.

Keywords: force sensor, haptic interface, differentiation, noise

1. Introduction

Switches mounted on product themselves or dedicated remote controllers belonging to specific products are generally used to operate electrical appliances in our daily lives. Operating devices with touch panels have also become popular [(1)–(3)], with smart phones being representative examples of such touch panels. Touch panels are used to operate a device, based on the positional information of fingers, which is acquired as the finger contacts the display. An advantage of this is that the operation can be performed intuitively. Products created by adding touch panels on household electric appliances or furniture have been studied and developed in the recent years. Switches or touch panels, however, have only two types of information, on/off and positional information respectively. This means that many more types of operations would be possible, if the information that devices can acquire from humans is increased.

The number of studies on interfaces that use force information in addition to positional information is being progressed, based on the perspective described above. Sugiura *et al.* developed "FuwaFuwa", which detects pressure and contact position by incorporating photoreflectors in a flexible object [(4)]. FuwaFuwa is advantageous in that it is capable of detecting both pressure and contact position by using photo-reflectors only. However, FuwaFuwa is constrained by the fact that the interfaces are limited to flexible materials. In the field of robotics, various tactile sensors of distributed array types have been studied [(5)–(9)]. Tactile sensing is a popular issue in robotics, because a tactile sense is believed to be a key to advanced robotic manipulation [(10)]. In some cases, tactile sensors are used to robots as a skin [(5)(7)(11)(12)]. A whole-body tactile sensing is enabled by using the tactile sensors. However, wiring is complicated because of these studies require a large number of sensors on the surface of the interfaces. There are also methods using external force observer for sensorless tactile sensing, while the contact position is fixed [(13)(14)]. Furthermore, studies using a camera have been progressed [(15)(16)]. The usage of a camera reduces the number of required sensors. On the other hand, such methods require space for projection.

The studies using a force sensor are also being carried out. Salisbury proposed a method that detects contact positions and contact force on an end-effector by using a six-axis force sensor [(17)]. Bicchi *et al.* expanded into a method that is also possible to detect contact positions and contact force on an elastic end-effector [(18)(19)]. Based on these studies, Iwata *et al.* developed a whole-body haptic interface using force sensors as interfaces [(20)(21)]. Although the whole-body haptic interface is capable of accurately detecting contact on interfaces, tactile sensors are used to determine contact on the contact surface. Therefore, wiring is complicated as with the tactile sensors of distributed array types. Kubo *et al.* developed a method estimating both the contact position and the external force on a planar end-effector based on the reaction torque observer [(22)].

Tsuji *et al.* have developed a whole-body tactile technology known as "Haptic Armor", which uses no additional sensors on the surface of the interface [(23)]. This technology detects the positional information and the force information simultaneously, with force sensors only, by using an equilibrium equation of force and moment as well as equations for expressing the shape of the end effector when an external force acts on an interface. This technology can be used to detect the above information, as long as the deformation of a material can be estimated, even when a flexible material is used as end-effectors [(24)]. They have also applied this

a) Correspondence to: Hiroyuki Kitamura. E-mail: s15mm217@mail.saitama-u.ac.jp
* Graduate School of Science and Engineering, Saitama University
255, Shimo-okubo, Sakura-ku, Saitama 338-8570, Japan

technology to “Haptic Desk”, which gives whole-body tactile senses to a desk, by attaching force sensors on the legs of the desk [25]. This technology can also be applied to existing desks. Therefore, a variety of objects around us, such as desks and other furniture or household electric appliances, can be interfaced.

The deterioration in the accuracy of the calculated positional information when the force acting on an interface is small, however, can be cited as an issue for this technology. This issue is critical in some cases because the force is small at the moments of touching and releasing always. A device can potentially perform a process that is different from the one intended and ordered by a human, when the accuracy of the positional calculation is low. Additionally, other conventional studies may suffer with the degradation of the accuracy of the contact point calculation by using with the small force.

In this paper, the authors extend the theory of the Haptic Desk by proposing a positional calculation that uses the differentiated force information as a method for accurately calculating positions even a small external force. Even with a small external force, there is a case that a time change of force is large. The proposal is to use the differentiated force in such a case. Theoretical development in this paper shows that the differentiated force can be substituted for the position estimation. A compendium of the conventional study [25] is provided first in Section 2. A compendium of the proposed method is provided in Section 3. The experimental equipment is described in Section 4, while an experimental evaluation of the proposed method is described in Section 5. Finally, a conclusion is provided in Section 6.

2. Compendium of Haptic Desk

The basis of Haptic Desk in the literature [25] is described first for this paper. Haptic Desk is supported with four force sensors as shown in Fig. 1. The point of action of external force and the external vector are calculated when the external force accrued on the desk. The equilibrium of force and the equilibrium of moment on the desk show the following at this time:

$$\boldsymbol{F}^e + \boldsymbol{F}^o = \boldsymbol{0} \cdots\cdots (1)$$

$$\boldsymbol{F}^e \times (\boldsymbol{P}^e - \boldsymbol{P}^o) + \boldsymbol{M}^o = \boldsymbol{0} \cdots\cdots (2)$$

$$\boldsymbol{F}^o = \sum_{i=1}^{n} \boldsymbol{F}_i^s$$

$$\boldsymbol{M}^o = \sum_{i=1}^{n} (\boldsymbol{F}_i^s \times (\boldsymbol{P}_i^s - \boldsymbol{P}^o)).$$

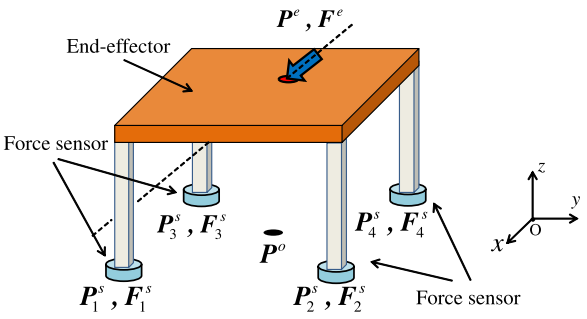

Fig. 1. Calculation of contact point

Here, $\boldsymbol{F}^e$ denotes the external force, $\boldsymbol{P}^e$ denotes the point of action of external force, and $\boldsymbol{P}^o$ denotes the reference position. And, n denotes number of supported points, $\boldsymbol{F}_i^s$ denotes force measured with the ith force sensor, $\boldsymbol{P}_i^s$ denotes position of the ith force sensor from the reference position, and $\boldsymbol{M}^o$ denotes the moment around the reference position respectively. Equation (2) can be rewritten as follows:

$$\begin{aligned} M_x^o &= F_z^e(P_y^e - P_y^o) - F_y^e(P_z^e - P_z^o) \\ M_y^o &= F_x^e(P_z^e - P_z^o) - F_z^e(P_x^e - P_x^o) \\ M_z^o &= F_y^e(P_x^e - P_x^o) - F_x^e(P_y^e - P_y^o) \end{aligned} \cdots\cdots (3)$$

$$\begin{aligned} P_x^e &= \frac{-M_y^o - F_x^e P_z^o}{F_z^e} + P_x^o + \frac{F_x^e}{F_z^e} P_z^e \\ &= \frac{M_z^o - F_x^e P_y^o}{F_y^e} + P_x^o + \frac{F_x^e}{F_y^e} P_y^e. \end{aligned} \cdots\cdots (4)$$

Equation (5) is shown from (1) and (4).

$$\begin{aligned} P_x^e &= \frac{M_y^o - F_x^o P_z^o}{F_z^o} + P_x^o + \frac{F_x^o}{F_z^o} P_z^e \\ &= \frac{-M_z^o - F_x^o P_y^o}{F_y^o} + P_x^o + \frac{F_x^o}{F_y^o} P_y^e \end{aligned} \cdots\cdots (5)$$

Here, subscripts x, y, and z show the direction of Cartesian coordinates. $\boldsymbol{F}^o$ and $\boldsymbol{M}^o$ in (5) are measured with the force sensors. Unknown variable is only $\boldsymbol{P}^e$, because $\boldsymbol{P}^o$ and $\boldsymbol{P}_i^s$ are known variables determined by the mechanism. Therefore, (5) yields a straight line parallel to the external force $\boldsymbol{F}^e$ like the broken line in Fig. 1. The form of the desk is regarded as the composition according to p pieces of plane surfaces, which are shown as follows:

$$f_k(\boldsymbol{P}^e) = 0 \quad (k = 1, 2, \cdots, p). \cdots\cdots (6)$$

The point of action of external force $\boldsymbol{P}^e$ is determined from the solution of simultaneous (5) and (6) when the external force accrued. Hereafter, the point of action of external force referred to as the contact point.

The error on the force/moment information depends on the offset of the force sensor, which varies with the weight of the desk with multiple goods on it. Since the arrangement of goods on the desk may change day by day, the offset needs to be calibrated at the beginning of the work. A DC offset is derived by the calibration with a low-pass filter and it is removed in the calibration. The calibration is performed for a fixed time just after starting force measurement. The calibration dose not require a manual operation because it is performed automatically after starting force measurement.

3. Proposed Method

3.1 Trial Calculation for Error of Contact Point

In the conventional method described in the preceding section, the equation of contact point calculation in (5) is used the force information measured with force sensors. Therefore, the error of the calculated contact point occurs if there is a sensor noise in the measured force. This phenomenon prominently occurs when the force is small. As the cause, a smallness of S/N ratio is pointed out. Especially, the error is large so that the sensor noise strongly affects, if force component in the denominator of (5) is near 0. F_z^o measured when the

external force is not applied to the force sensors, shows maximum 0.4 N amplitude of the sensor value. It is supposed as the noise included in sensor values. Here, the authors regard as a position, distanced 0.2 m in x-axis direction from the center of the desk, is applied by external force constituted $F_z^e = -2$ N, $F_x^e = 0$ N, and $F_y^e = 0$ N. The contact point $P_x^{e\prime}$ calculated using in (5), is shown in the following equation:

$$P_x^{e\prime} = \frac{M_y^i}{F_z^o}. \cdots (7)$$

Here, M_y^i indicates that the moment around the reference position is an ideal value which is not included any noises. The measured value of F_z^o taken into consideration sensor noises is 1.6–2.4 N. $P_x^{e\prime}$ are calculated 0.17 m and 0.25 m respectively if the values of $F_z^o = 1.6$ N and $F_z^o = 2.4$ N are substituted in (7). Considering $P_x^e = 0.2$ m, the calculated values of $P_x^{e\prime}$ include an error. The error range for P_x^e is 0–0.083 m. Then, the error range becomes wider when force is small since (7) shows inverse relationship.

The conventional method has used a quadratic low-pass filter after obtaining the force information, and the maximum amplitude of noise has been able to attenuate 0.024 N. However the error has not disappeared because it is not possible to remove all of the noise. Therefore, in this paper, the authors propose the method which calculated the contact point by using the differentiated force information instead of the force information.

3.2 Contact Point Calculation using Differentiated Force Information There is the error of the calculated contact point in the conventional method when the force is small, as shown in Section 3.1. The moments occurring the small force corresponds the moments of touching and releasing on the desk. In this study, the authors propose the usage of the differentiated force information in order to decrease the error occurring at the above two moments.

In this study, the equation of the differentiation is given as follows:

$$f'(t) = \frac{f(t) - f(t - nT_s)}{nT_s}. \cdots (8)$$

t denotes the present time, and T_s denotes the sampling time of the force sensor. $f(t)$ and $f'(t)$ denote the measured value of the force sensor and the value of differentiated force respectively. n denotes the constant integer and determines the time interval corresponding the denominator of (8).

Additionally, a pseudo differential is used for the calculation of the differentiation in this study. The pseudo differential is as follows.

- The value of differentiated force is calculated by (8).
- The noise of the differentiated force is decreased with the low-pass filter.

The natural frequency of the desk may induce the resonance. Therefore, the cut-off frequency of the low-pass filter needs to be set smaller than the natural frequency of the desk. The natural frequency of the desk is 5.9 Hz and the cut-off frequency of the low-pass filter in the pseudo differential is set 4.77 Hz. Then, the frequency bandwidths of touching and releasing force are limited by the cut-off frequency. However, the touching and releasing motions are hardly influenced by the limitation because the difference between the bandwidths of the cut-off frequency and the natural frequency is not large.

The equation using a differentiated force is given by (1) and (2) as follows:

$$\dot{\boldsymbol{F}}^e + \dot{\boldsymbol{F}}^o = \boldsymbol{0} \cdots (9)$$

$$\dot{\boldsymbol{F}}^e \times (\boldsymbol{P}^e - \boldsymbol{P}^o) + \boldsymbol{F}^e \times (\dot{\boldsymbol{P}}^e - \dot{\boldsymbol{P}}^o) + \dot{\boldsymbol{M}}^o = \boldsymbol{0}. \cdots (10)$$

$\dot{\boldsymbol{F}}^e$ denotes the value of the differentiated external force, $\dot{\boldsymbol{F}}^o$ denotes the differentiated value of the total force applied on supported points, and $\dot{\boldsymbol{M}}^o$ denotes the value of the differentiated moment around the reference position. $\dot{\boldsymbol{P}}^e$ denotes the value of the differentiated contact point, and $\dot{\boldsymbol{P}}^o$ denotes the value of the differentiated reference position. $\boldsymbol{P}^o$ is the constant value, which means $\dot{\boldsymbol{P}}^o = \boldsymbol{0}$. (10) is used when the external force is small. Then, the second term in (10) is also small. Therefore, the second term in (10) can be neglected unless the time change of the contact point is not considerably large. Here, assuming that the time change of the contact point at the moments of touching and releasing on the desk is not considerably large, the second term in (10) can be neglected. Then, (11) and (12) are obtained.

$$\dot{\boldsymbol{F}}^e \times (\boldsymbol{P}^e - \boldsymbol{P}^o) + \dot{\boldsymbol{M}}^o = \boldsymbol{0} \cdots (11)$$

$$\begin{aligned} P_x^e &= \frac{\dot{M}_y^o - \dot{F}_x^o P_z^o}{\dot{F}_z^o} + P_x^o + \frac{\dot{F}_x^o}{\dot{F}_z^o} P_z^e \\ &= \frac{-\dot{M}_z^o - \dot{F}_x^o P_y^o}{\dot{F}_y^o} + P_x^o + \frac{\dot{F}_x^o}{\dot{F}_y^o} P_y^e \cdots (12) \end{aligned}$$

The value of the differentiated force is greater, if there is a time change of the force when the external force occurred on the desk. The trial calculation of the errors produced by the sensor noise is done in a manner similar to Section 3.1 from the results of preliminary experiment. The mean time change of force of five subjects were −45 N/s in z-axis direction at the moment of touching on the desk. On the other hand, the maximum amplitude of the noise was 0.024 N with a low-pass filter. Therefore, a typical example of F_z^o is depicted by the following equation:

$$F_z^o = -45t + 0.024\lambda(t) \quad -1 \le \lambda(t) \le 1. \cdots (13)$$

t denotes a time, and $\lambda(t)$ denotes the function simulating the noise. By differentiating (13) shows the following equation:

$$\dot{F}_z^o = -45 + 0.024\dot{\lambda}(t). \cdots (14)$$

The noise is often amplified by differentiating. Here, the amplification degree of differentiated force against force was calculated based on the results of the preliminary experiment. Maximum amplitude of the differentiated noise was 0.29 N/s. Hence (14) can be reformed as follows:

$$\dot{F}_z^o = -45 + 0.29\eta(t) \quad -1 \le \eta(t) \le 1. \cdots (15)$$

$\eta(t)$ denotes the function simulating the differentiated noise. A contact point $P_x^{e\prime\prime}$ utilizing the differentiated force information is given by (7) and (12) as follows:

$$P_x^{e\prime\prime} = \frac{\dot{M}_y^i}{\dot{F}_z^o}. \cdots (16)$$

The error range of $P_x^{e\prime\prime}$ is 0–0.0026 m by using (15) and (16).

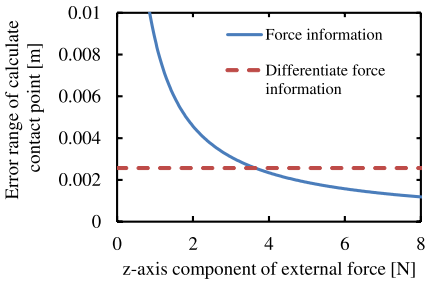

Fig. 2. Comparison of error of contact point calculation

Here, the error ranges of $P_x^{e\prime}$ and $P_x^{e\prime\prime}$ were compared by using (13) and (15). The result is shown in Fig. 2. The error of contact point using the differentiated force information is smaller than using force information when $F_z^e \leq 3.8\,\mathrm{N}$ as revealed in Fig. 2. Therefore, there are some cases that the accuracy of contact point calculation using the differentiated force information is high compared with the force information, if the amplification degree of $\dot{\lambda}(t)$ is not great. Additionally, the difference between the each error range in Fig. 2 is especially influenced by the form of the equation of the contact point calculation. In the conventional method, when the magnitude of F_z^o in the denominator of (7) is small, the value of the denominator of (7) may become a minute value by the noise. Then, the large error occurs. In the proposed method, if the differentiated force information is used for the contact point calculation, the value of the denominator of the equation become a large value as shown (15) and (16). If this value is as large as the value which does not become a minute value by the sensor noise amplified by the differentiation, using (16) prevents the occurrence of the error. Setting a large time interval than the sampling time of the force sensor in (8) prevents the amplification of the noise and gets a large time change of the force. Hence, this time interval is set 166 ms (n = 200, T_s = 0.83 ms) from the preliminary experiment.

3.3 Using Force Information and Differentiated Force Information Properly The contact point includes the large error when force is small as detailed in Section 3.1. Therefore, the authors propose the method using the force information and the differentiated force information properly by the condition of the magnitude of the force. As the method above, it is believed that the highly accurate calculation of the contact point is possible regardless of the magnitude of the force. In this study, the contact points calculated by using the force information and the differentiated force information respectively are compared at the moments of touching and releasing. And the authors examine the validity of the differentiated force information in the case when force is small by the comparison results. If the validity is confirmed, the threshold value of force in order to use the two information properly is derived. At this time, the threshold value of force is derived in each moment.

The mechanism of the contact point calculations using the force information and the differentiated force information properly, is shown in Fig. 3. First of all, the force information obtained with force sensors is converted the differentiated value. Subsequently, the contact candidate point $\boldsymbol{P}_r^e$ using the force information and the contact candidate point $\boldsymbol{P}_d^e$ using the differentiated force information, are calculated

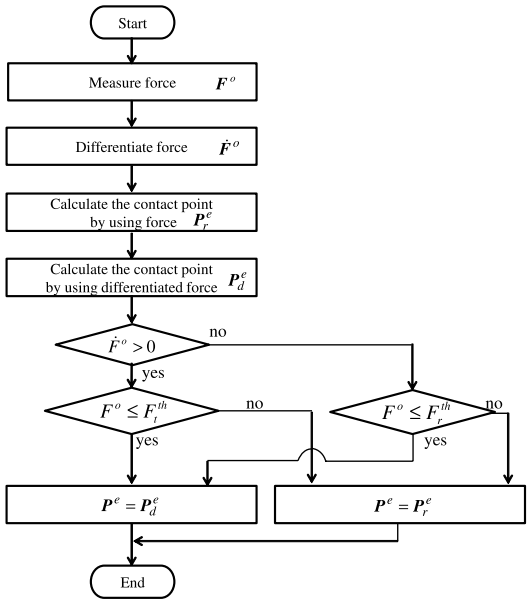

Fig. 3. Switch force information and differentiated force information

(a) (b)

Fig. 4. Appearance of Haptic Desk. (a) Haptic Desk. (b) Force sensor

respectively. The input motion is determined by the sign of the value of differentiated force after calculating the candidate points. After determining the input motion, the contact point is calculated by comparing the measured force and the threshold value of force derived experimentally in advance. Here, the threshold values at the moments of touching and releasing, are referred to as F_t^{th} and F_r^{th} respectively. $\boldsymbol{P}_d^e$ calculated using the differentiated force information is determined as the contact point $\boldsymbol{P}^e$, if the magnitude of the input force F^o is the threshold value and below. $\boldsymbol{P}_r^e$ calculated using the force information is determined as $\boldsymbol{P}^e$, if F^o is the threshold value and over.

4. Experimental Equipment

The experimental equipment is shown in Fig. 4. The desk is a commercial product, and the four six-axis force sensors are attached to the desk legs. The size of the desk is shown in Fig. 5 and Table 1. The top board and the desk shelf of the desk are made of a medium density fiberboard, and the side frame is made of a steel. The parameters of six-axis force sensor are shown in Table 2. The information obtained from the four six-axis force sensors is sent to a notebook computer, and the contact point is calculated using the

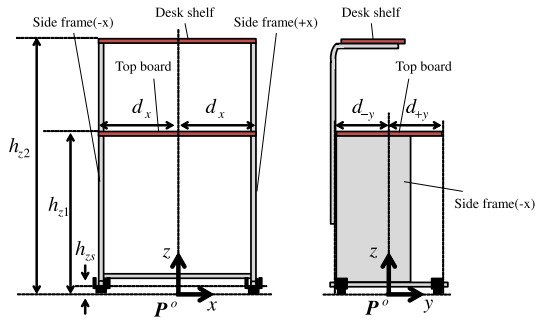

Fig. 5. Schematic diagram of Desk

Table 1. Parameters of Haptic Desk

ω^c	Weight of the desk	13.7 kg
d_x	Distance from the center to the top board edge	0.375 m
d_{+y}	Distance from the center to the top board edge	0.250 m
d_{-y}	Distance from the center to the top board edge	0.250 m
d_{z1}	Height from the sensor device to the top board	0.733 m
d_{z2}	Height from the sensor device to the desk shelf	1.20 m
h_{zs}	Height from the sensor device to the bottom of the side frame	0.0280 m

Table 2. Parameters of force sensor

Rated capacity	F_z	±300 N
	F_x, F_y	±150 N
	M_x, M_y, M_z	±4 Nm
Allowable load		±150% R.O.
Nonlinearity		±1.5% R.O.
Other axis interference		±2.0% R.O.
Output frequency		1200 kHz
Resolution		1/2000

program in the notebook computer. Besides, the condition for the contact point calculation in conventional method [25] is determined $F^o \geq 2$ N. Therefore, the condition is adopted for this paper too.

5. Experiment

5.1 Verification on Accuracy of Contact Point Calculation using the Force Information and the Differentiated Force Information Respectively

In this paper, the contact candidate points, $\boldsymbol{P}_r^e$ and $\boldsymbol{P}_d^e$, calculated using the force information and the differentiated force information respectively, were compared first at the moments of touching and releasing. A threshold value of force by using the proposed method was derived, based on the result of the comparison. Seven subjects whose age is 21–23 years old participated in this experiment.

The contact candidate points, $\boldsymbol{P}_r^e$ and $\boldsymbol{P}_d^e$, calculated using the force information and the differentiated force information respectively, were compared first. Nine points of action of external forces were set on the top board of the desk as shown in Fig. 6. A motion involved touching and releasing a point (hereinafter referred to as press motion) was performed three times on each point by three test subjects. A single data was comprised of the results obtained after one test subject performed the press motion on a single point of action once. The center of the point of action in Fig. 6, p_5 was at $x = 0.0$ m and $y = 0.0$ m, with the distances between each point being $d_a = 0.3$ m and $d_b = 0.2$ m. The point-to-point distance from the center of the top board ($x = 0.0$ m and $y = 0.0$ m) to each point of action is referred to as D_t, while the point-to-point distances to the candidate contact points of $\boldsymbol{P}_r^e$ and $\boldsymbol{P}_d^e$ are

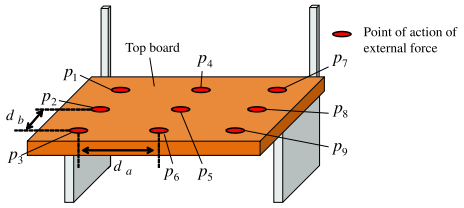

Fig. 6. Setting points of action of external force

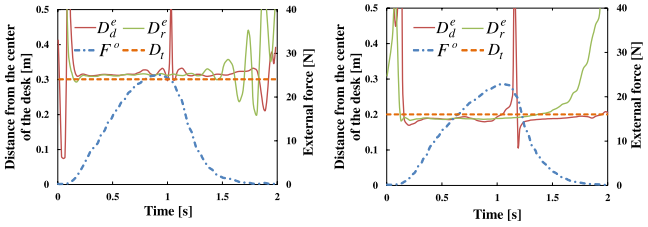

Fig. 7. Time response of D_r^e and D_d^e. (a) When contacting p_8. (b) When contacting p_6

referred to as D_r^e and D_d^e, respectively. Therefore, the point-to-point distance D_t to the point of action p_3 is 0.36 m. Examples of the magnitude of the external force F^o, as well as the point-to-point distances D_r^e and D_d^e when one test subject performed a press motion, is shown in Fig. 7. At the moment of touching on the desk and F^o became greater, the point-to-point distance D_r^e using the force information converged at 0.22 s, and the point-to-point distance D_d^e using the differentiated force information converged at 0.18 s respectively as shown in Fig. 7(a). The point-to-point distance D_d^e using the differentiated force information converged earlier than the point-to-point distance D_r^e using the force information. At the moment of releasing from the desk and F^o became smaller, the point-to-point distance D_r^e using the force information diverged, but the point-to-point distance D_d^e using the differentiated force information did not diverge and remained constant. Next, at the moment of releasing from the desk and F^o became smaller, the point-to-point distance D_r^e using the force information resulted in diverging as shown in Fig. 7(b), similar to Fig. 7(a). At the moment of touching on the desk and F^o became greater, the point-to-point distance D_r^e using the force information, converged at 0.14 s and the point-to-point distance D_d^e using the differentiated force information converged at 0.35 s respectively. The point-to-point distance D_d^e using the differentiated force information therefore converged later, unlike the case depicted in Fig. 7(a). The result, indicating that the point-to-point distance D_r^e using the force information diverged when the external force became weaker, was obtained with data from other test subjects and points of action as well. At the moment of touching on the desk, there were both cases of the values of the point-to-point distance D_d^e using the differentiated force information converging earlier and later. Therefore, there was a result that the accuracy of contact point calculation varied. Furthermore, the point-to-point distance D_d^e using the differentiated force information fluctuated significantly in the vicinity of the maximum value for the magnitude of the external force F^o as shown in Figs. 7(a) and (b). This was caused by the small S/N ratio due to the small value of the differentiated force.

The variance in D_r^e using the force information and D_d^e

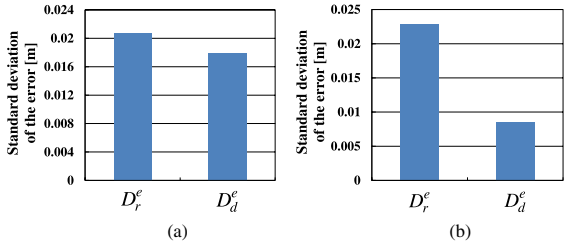

Fig. 8. Standard deviation of error of D_r^e and D_d^e. (a) When force increasing. (b) When force decreasing

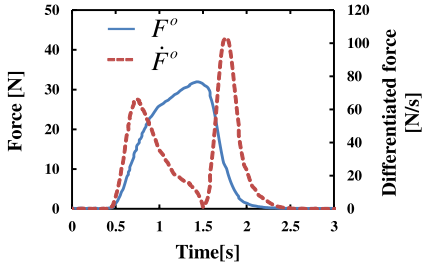

Fig. 9. Time response of F^o and $\dot{F}^o$

using the differentiated force information, when the external force was small, was compared next. The data of all test subjects and all points of action (81 pieces of data) were used to measure the standard deviation of errors with point-to-point distances D_r^e and D_d^e with respect to D_t at respective points of action. The maximum value of the magnitude F_{max} of the external force F^o, applied by the test subject during the experiments, was 20 N and higher as shown in Fig. 7. Similar results were obtained from other test subjects as well. Therefore, this study defines $2\,\mathrm{N} \leq F^o \leq 3\,\mathrm{N}$ as the condition for a small force, which indicates that the magnitude of the external force F^o is sufficiently smaller than the maximum value F_{max}. The mean values for D_r^e and D_d^e were calculated respectively. Next, the errors of D_r^e and D_d^e were calculated by difference between the derived means and D_t. And the standard deviation of the errors were compared. The results are shown in Fig. 8. The standard deviation of the error of D_d^e using the differentiated force information was reduced in comparison with D_r^e using the force information at the both moments of touching and releasing. The reduction rate in the standard deviation was different at the moments of touching and releasing.

There were several occasions where the accuracy of contact point calculation using the differentiated force information was low at the moment of touching on the desk, from the above results. The time response of the magnitude of external force F^o when the press motion was performed on the desk, as well as the value of the differentiated external force $\dot{F}^o$, are shown in Fig. 9. The value for the differentiated force at the moment of touching, was smaller in comparison to the moment of releasing from the desk, as depicted in Fig. 9. The accuracy of the contact point calculation using the differentiated force information was low at the small value of the differentiated force. Furthermore, the maximum values for the differentiated force at the moments of touching and releasing, was compared. The result indicated that a larger maximum values for the differentiated force were obtained at the moment of releasing from the desk 63 times out of 81 times,

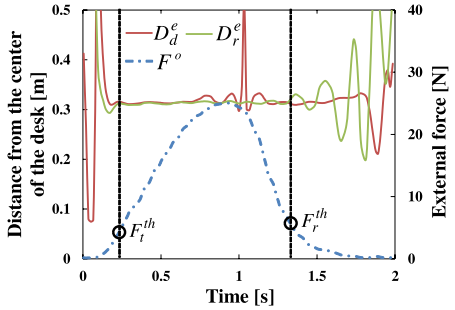

Fig. 10. Calculation example of F_t^{th} and F_r^{th}

which meant the probability was 77.8%. The time change of force was generally greater the moment of releasing than the moment of touching on the desk for that reason, which is believed to have led to the results shown in Fig. 7 and Fig. 8.

5.2 Deduction of Threshold Value for Selecting Force Information and Differentiated Force Information

The accuracy of the contact point calculation using the differentiated force information was confirmed to be greater than using the force information, when the force was small, as revealed by the results of Section 5.1. The threshold of force that serves as a condition for selecting the two types of information, was derived next. The accuracy of the contact point calculation using the differentiated force was greater the moment of releasing than the moment of touching on the desk. Therefore, separate threshold values were derived at the moments of touching and releasing for the purpose of this paper.

An example of how the threshold values were derived, is shown in Fig. 10. The method for deriving the threshold value F_t^{th} at the moment of touching is described first. The results obtained in Section 5.1 indicated that D_d^e using the differentiated force information converged later than D_r^e using the force information, at the moment of touching. The error of the contact point calculation can therefore potentially increase, when the differentiated force information is used after D_r^e using the force information has converged. The magnitude of the external force F^o at the instant when the time response of D_r^e using the force information has converged, was set to the threshold value F_t^{th}, in order to prevent the error described above. $|\dot{D}_r^e| \leq 0.2$ m/s was set as a condition for determining that D_r^e had converged. This condition was determined by the results of the preliminary experiments which the time change of $|\dot{D}_r^e|$ using the differentiated force information is converged within 0.2 m/s after touching on the desk. $F_t^{th} = 4.4$ N is shown in Fig. 10. The method for deriving the threshold value F_r^{th}, used at the moment of releasing from the desk, is described next. When the external force became weaker, D_r^e using the force information was diverged as described in Section 5.1. Therefore, the magnitude of the external force at the instant when D_r^e using the force information started to diverge, was set to the threshold value F_r^{th}. $|D_r^e - D_d^e| \geq 0.01$ m was set as a condition for determining the instant when D_r^e started to diverge. This condition was determined by the results of the preliminary experiments which the difference between the point-to-point distances using the force information and the differentiated force information is within 0.01 m just before releasing on the desk. $F_r^{th} = 5.1$ N is shown

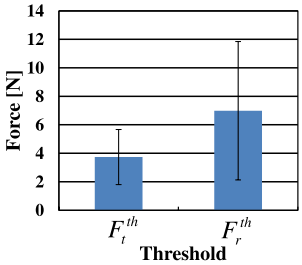

Fig. 11. Calculated values of F_t^{th} and F_r^{th}

in Fig. 10.

An experiment similar to the one described in Section 5.1 was conducted with five test subjects, based on the conditions described above. The data collected from all test subjects for all points of action (135 pieces of data) were used to derive the mean values and standard deviations of the threshold values F_t^{th} and F_r^{th} respectively, at the moments of touching and releasing.

The mean for the threshold values and the standard deviations of F_t^{th} and F_r^{th} are shown in Fig. 11. The mean for the threshold values for F_t^{th} and F_r^{th} were 3.74 N and 6.98 N respectively. Taking into consideration the standard deviations, the threshold values of F_t^{th} and F_r^{th} were 1.80–5.67 N and 2.12–11.8 N respectively. It is difficult to set a unique threshold when the variance is significant. In order to evaluate the derived threshold values, means for the threshold values and the two values with which the deviation with respect to the mean values was maximum as shown in Fig. 11, were compared as the candidates for the threshold value. The conditions of the force for the contact point calculation in the conventional method [25] was taken into consideration in this experiment. The force whose magnitude is smaller than 2 N, is not considered the threshold value. The candidates of the threshold value F_t^{th}, therefore, were two values of 3.74 N and 5.67 N. And the candidates of the threshold value F_r^{th}, were the three values of 2.12 N, 6.98 N and 11.8 N. The calculated contact points using each of the candidates of the threshold value described above, were compared as the evaluation of the candidates of the threshold value. There were four test subjects, who were asked to perform press motions on the points of action on the top board of the desk, as with the previous experiment.

The comparisons at the moments of touching and releasing are shown respectively in Fig. 12. The horizontal axis indicates the conventional method and the proposed method using candidates of respective threshold values. The vertical axis indicates the standard deviations of errors of the point-to-point distances according to the conventional method and the proposed method with respect to the individual points of action. The standard deviations reached minimum when F_r^{th} = 5.67 N at the moment of touching on the desk, according to the graphs of respective test subjects. There was a reduction of standard deviation compared to the conventional method in this instance, by 3.26%, 1.35%, 4.89% and 0.861% with test subjects 1 to 4, respectively. The standard deviation was minimal when F_r^{th} = 11.8 N at the moment of releasing from the desk. There was a greater reduction of standard deviation compared to the conventional method in this instance, which exceeded the threshold value F_t^{th} at the moment of touching

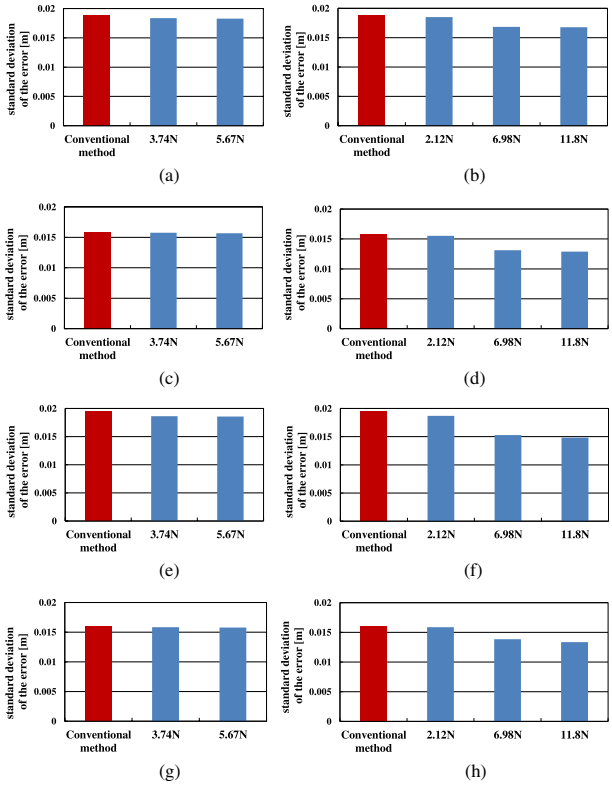

Fig. 12. Evaluation F_t^{th} and F_r^{th}. (a) F_t^{th} with subject 1. (b) F_r^{th} with subject 1. (c) F_t^{th} with subject 2. (d) F_r^{th} with subject 2. (e) F_t^{th} with subject 3. (f) F_r^{th} with subject 3. (g) F_t^{th} with subject 4. (h) F_r^{th} with subject 4

on the desk, by 11.0%, 16.4%, 24.1% and 18.5% with test subject 1 to 4, respectively. The accuracy for the contact point calculation according to the proposed method was highest when the threshold value was set to the maximum value, with consideration for the standard deviation.

5.3 Verification on Accuracy for Contact Point Calculation for using Force Information and Differentiated Force Information Comparisons were performed between the conventional method [25] and the proposed method using the derived threshold value in the Section 5.2. The threshold values were set to F_t^{th} = 5.67 N and F_r^{th} = 11.8 N. The results are shown in Fig. 13. The calculated contact points by the proposed method converged on the points of action of external force. The time constants of the convergence were shorter compared to the ones by the conventional method. The mean error and the standard deviation in Fig. 13 are shown in Fig. 14. Both the mean error and the standard deviation were smaller with the proposed method than the conventional method. In this experiment, the validity of the proposed method was also confirmed with another desk whose structure is different from the one in Fig. 5.

Next, a test subject was asked to trace the Japanese character “kita” with a finger on the top board of the desk, and the contact points were calculated using the conventional method and the proposed method simultaneously for comparison. In this experiment, the contact point calculation by the differentiated force information is used the starting and termination of each stroke in the word due to the moments of touching and releasing on the desk. The contact point calculation of

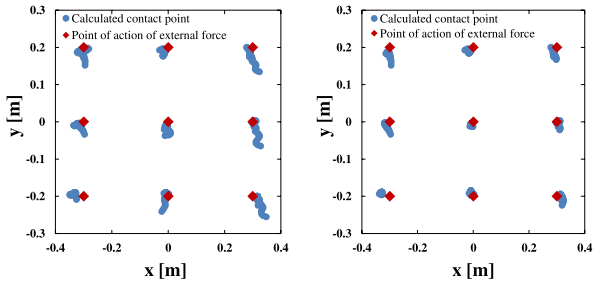

Fig. 13. Contact point comparison. (a) Conventional method. (b) Proposed method

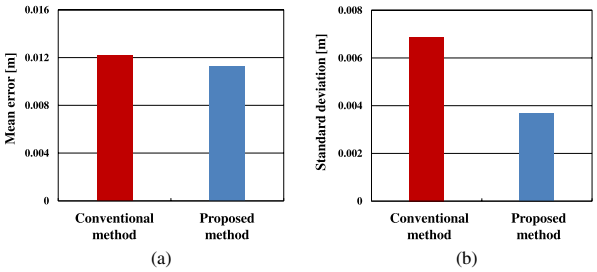

Fig. 14. Evaluation of calculated contact point (a) Mean error. (b) Standard deviation

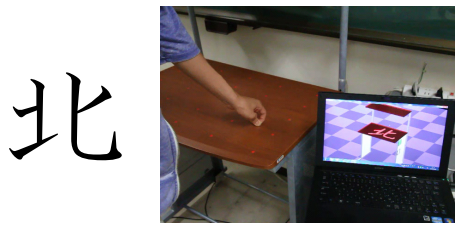

Fig. 15. Condition of experiment drawing word. (a) Japanese character “kita”. (b) Experiment landscape

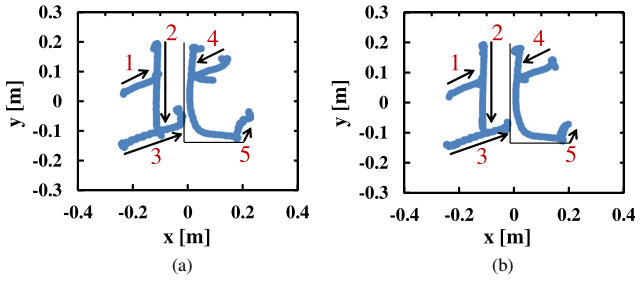

Fig. 16. Comparison when drawing word. (a) Conventional method. (b) Proposed method

the trace motion between the starting and termination is used only the force information. The large force is applied during the trace motion, which do not require the differentiated force information. The condition of the experiment and the results are shown in Fig. 15 and Fig. 16 respectively. The arrows and numbers indicated in Fig. 16(a) and (b) represent the directions and sequence of the character as it was traced. The average velocity of tracing the character in Fig. 16 was 3.37±0.644 cm/s. In the conventional method, errors occurred in the contact point where the tracing of each line terminated as shown in Fig. 16. The proposed method, on the other hand, reduced the error compared with the conventional method. The standard deviation at the moments of touching

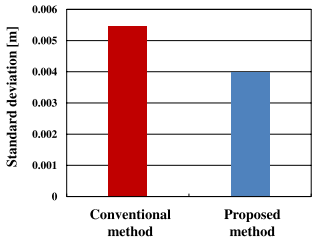

Fig. 17. Evaluation of the moments of the touching and releasing in each line of character

and releasing in each line of the character is shown in Fig. 17 as a quantitative rating. Using the assumption that the time change of the contact point at the moments of touching and releasing is not considerably large, the standard deviation in Fig. 17 is related to the error of the calculated contact point. The above results indicated the accuracy of the contact point calculation was improved by using the proposed method.

6. Conclusion

This paper has described the development of a method for Haptic Desk with the accurate contact point calculation using the force information and the differentiated force information properly. The experimental results have indicated that the accuracy of the contact point calculation using the differentiated force information was higher than the one using the force information when external force was small. Besides, the standard deviations of the contact point calculation using the proposed method have been reduced. From the above results, it was confirmed the improved accuracy of the contact point calculation in haptic interface.

Acknowledgment

This study was supported in part by the Grant-in-Aid for Scientific Research (B), Number 16H04311.

References

(1) J. Colegrove: “The state of the touch-screen market in 2010”, *Information Display*, Vol.26, No.3, pp.22–24 (2010)
(2) S. Kim, W. Choi, W. Rim, Y. Chun, H. Shim, H. Kwon, J. Kim, I. Kee, S. Kim, S. Lee, and J. Park: “A highly sensitive capacitive touch sensor integrated on a thin-film-encapsulated active-matrix OLED for ultrathin displays”, *IEEE Trans. Electron Devices*, Vol.58, No.10, pp.3609–3615 (2011)
(3) C. Lin, Y. Chang, C. Hung, C. Tu, and C. Chuang: “Position estimation and smooth tracking with a fuzzy logic-based adaptive strong tracking kalman filter for capacitive touch panels”, *IEEE Trans. Industrial Electronics* (2015)
(4) Y. Sugiura, G. Kakehi, A. Withana, C. Lee, D. Sakamoto, M. Sugimoto, M. Inami, and T. Igarashi: “Detecting shape deformation of soft objects using directional photoreflectivity measurement”, in Proc. Annu. ACM Symposium on User Interface Software and Technology, pp.508–516 (2011)
(5) Y. Ohmura, Y. Kuniyoshi, and A. Nagakubo: “Conformable and scalable tactile sensor skin for curved surfaces”, *IEEE Int. Conf. on Robotics and Automation*, pp.1348–1353 (2006)
(6) K. Suwanratchatamanee, M. Matsumoto, and S. Hashimoto: “Robotic tactile sensor system and applications”, *IEEE Trans. Industrial Electronics*, Vol.57, No.3, pp.1074–1087 (2010)
(7) T. Sagisaka, Y. Ohmura, Y. Kuniyoshi, A. Nagakubo, and K. Ozaki: “High-density conformable tactile sensing glove”, IEEE Int. Conf. on Humanoid Robots, pp.537–542 (2011)
(8) P. Peng and R. Rajamani: “Flexible micro-tactile sensor for normal and shear elasticity measurements”, IEEE Trans. Industrial Electronics, Vol.59, No.12, pp.4907–4913 (2012)
(9) S. Yun, S. Park, B. Park, Y. Kim, S. Park, S. Nam, and K. Kyung: “Polymer-waveguide-based flexible tactile sensor array for dynaqmic response”, Advanced Materials, pp.4474–4480 (2014)

(10) J. Tegin and J. Wikander: "Tactile sensing in intelligent robotic manipulation-a review", *Industrial Robot*, Vol.32, No.1, pp.64–70 (2005)
(11) T. Hoshi and H. Shinoda: "A tactile element based on nonlinear elasticity to sense contact area", Proc. IEEJ 22nd Sensor Symposium, pp.375–379 (2005)
(12) A. Schmitz, P. Maiolino, M. Maggiali, L. Natale, G. Cannata, and G. Metta: "Methods and technologies for the implementation of large-scale robot tactile sensors", *IEEE Trans. Robotics*, Vol.27, No.3, pp.389–400 (2011)
(13) T. Murakami, R. Nakamura, F. Yu, and K. Ohnishi: "Force sensorless impedance control by disturbance observer", in Proc. Power Conversion Conf., pp.352–357 (1993)
(14) T. Murakami, F. Yu, and K. Ohnishi: "Torque sensorless control in multidegree-of-freedom manipulator", *IEEE Trans. Industrial Electronics*, Vol.40, No.2, pp.259–265 (1993)
(15) Y. Sun, J. Hollerbach, and A. Mascaro: "Estimation of fingertip force direction with computer vision", IEEE Trans. Robotics, Vol.25, No.6, pp.1356–1369 (2009)
(16) K. Sato, K. Kamiyama, N. Kawakami, and S. Tachi: "Finger-shaped gelforce: sensor for measuring surface traction fields for robotic hand", *IEEE Trans. Haptics*, Vol.3, No.1, pp.37–47 (2010)
(17) J. Salisbury: "Interpretation of contact geometries from force measurements", in Proc. IEEE Int. Conf. on Robotics and Automation, pp.240–247 (1984)
(18) A. Bicchi: "Intrinsic contact sensing for soft fingers", in Proc. IEEE Int. Conf. on Robotics and Automation, pp.968–973 (1990)
(19) A. Bicchi, J. Salisbury, and D.L. Brock: "Contact sensing from force and torque measurements", *Int. J. Robotics Research*, Vol.12, No.3, pp.249–262 (1993)
(20) H. Iwata and S. Sugano: "Whole-body covering tactile interface for human robot coordination", in Proc. IEEE Int. Conf. on Robotics and Automation, pp.3814–3824 (2002)
(21) H. Iwata and S. Sugano: "Human-robot-contact-state identification based on tactile recognition", *IEEE Trans. Industrial Electronics*, Vol.52, No.6, pp.1468–1477 (2005)
(22) R. Kubo and K. Ohnishi: "Attitude control of planar end-effector and estimation of contact point using parallel mechanism", *IEEJ Trans. IA*, Vol.126, No.9, pp.1243–1250 (2006)
(23) T. Tsuji, Y. Kaneko, and S. Abe: "Whole-body force sensation by force sensor with shell-shaped end-effector", *IEEE Trans. Industrial Electronics*, Vol.56, No.5, pp.1375–1382 (2009)
(24) N. Kurita, H. Hasunuma, S. Sakaino, and T. Tsuji: "Simplified whole-body tactile sensing system using soft material at contact areas", in Proc. IEEE Int. Conf. on Industrial Electronics Society, pp.4264–4269 (2013)
(25) T. Tsuji and S. Sakaino: "Haptic signal processing of a desk-type interface using force sensors", in Proc. IEEJ Int. Workshop on Sensing, Actuation, and Motion Control, IS4-5 (2015)

Hiroyuki Kitamura (Non-member) received the B.E. degree in electrical and electronic systems engineering from Saitama University, Saitama, Japan, in 2015. He is currently working on M.E. degree at the Department of Electrical and Electronic Systems, Saitama University. He is engaged in research on haptics.

Sho Sakaino (Senior Member) received the B.E. degree in system design engineering and the M.E. and Ph.D. degrees in integrated design engineering from Keio University, Yokohama, Japan, in 2006, 2008, and 2011, respectively. He is currently an assistant professor with the Department of Electrical and Electronic Systems, Saitama University, Saitama, Japan. He received IEEJ Industry Application Society Distinguished Transaction Paper Award in 2011. His research interests include mechatronics, motion control, robotics, and haptics.

Toshiaki Tsuji (Senior Member) received the B.E. degree in system design engineering and the M.E. and Ph.D. degrees in integrated design engineering from Keio University, Yokohama, Japan, in 2001, 2003, and 2006, respectively. He was a research associate in Department of Mechanical Engineering, Tokyo University of Science from 2006 to 2007. He is currently an Associate Professor in Department of Electrical and Electronic Systems, Saitama University. His research interests include motion control, haptics and rehabilitation robot. He received the FANUC FA and Robot Foundation Original Paper Award in 2007 and 2008.